

# New Design Topology of High- $Q$ Factor Printed Base Antenna Having Unequal Width and Pitch Used for Near-Field Wireless Power Transmission

Jinhyoung Kim<sup>1</sup>, Student Member, IEEE, Cheolung Cha, Jungsuek Oh<sup>2</sup>, Senior Member, IEEE, and Yongtaek Hong<sup>3</sup>, Member, IEEE

**Abstract**—In this article, an unequal printed structure is proposed to obtain high quality factor ( $Q$ -factor) coil antenna in wireless power transmission systems. In the resonance method wireless power transmission, the  $Q$ -factor is one of the important factors that determine the transmission efficiency. Generally, the  $Q$ -factor is increased by increasing the size of the resonator, but, through the structure presented in this article, the  $Q$ -factor can be maximized without changing the size. In addition, this method can improve the low  $Q$ -factor of the “printed antenna,” which was pointed out as a disadvantage. The main idea to achieve a high  $Q$ -factor is that pitch and width are not constant along the width. The line pitch and width of the printed pattern are gradually increased in proportion with the outer diameter. By using this design method, the  $Q$ -factor is increased about 21.8% in comparison with the conventionally designed antenna. In addition, it can be confirmed that the antenna performance is substantially superior to that of a typical coil antenna if the size conditions are the same.

**Index Terms**—High quality factor ( $Q$ -factor), printed base resonator, unequal form factor, wireless power transmission.

## I. INTRODUCTION

TODAY, a 6.78-MHz antenna, also called a resonance antenna, is studied to apply to the wireless power transmission system. Almost 6.78-MHz resonance antennas have a similar shape with the inductor to form a magnetic field around the coil. The first resonance antenna invented by MIT had a solenoid structure. However, nowadays, most of the antennas have a spiral structure, as shown in Fig. 1. Most of them are made by a circular coil. However, this circular coil antenna is not good for common use manufactured because

Manuscript received February 2, 2021; revised April 2, 2021 and June 11, 2021; accepted July 18, 2021. Date of publication July 30, 2021; date of current version February 3, 2022. This work was supported by the Korea Industrial Technology Promotion Agency (KIAT) with the funds of the Ministry of Trade, Industry and Energy through the Safety Technology Commercialization Platform Construction Project under Grant P0003951 and the Project of High-Tech Textile Material Prototyping and Commercialization under Grant B0080325001923. Recommended for publication by Associate Editor Debaprasad Kastha. (Corresponding author: Yongtaek Hong.)

Jinhyoung Kim, Jungseok Oh, and Yongtaek Hong are with the Department of Electrical and Computer Engineering, Seoul National University, Seoul 08826, South Korea (e-mail: kimjh91@keti.re.kr; yongtaek@snu.ac.kr; jungsuek@snu.ac.kr).

Cheolung Cha is with Korea Electronics Technology Institute, Seongnam-si 13509, South Korea (e-mail: cucha@keti.re.kr).

Color versions of one or more figures in this article are available at <https://doi.org/10.1109/JESTPE.2021.3101477>.

Digital Object Identifier 10.1109/JESTPE.2021.3101477

2168-6777 © 2021 IEEE. Personal use is permitted, but republication/redistribution requires IEEE permission. See <https://www.ieee.org/publications/rights/index.html> for more information.

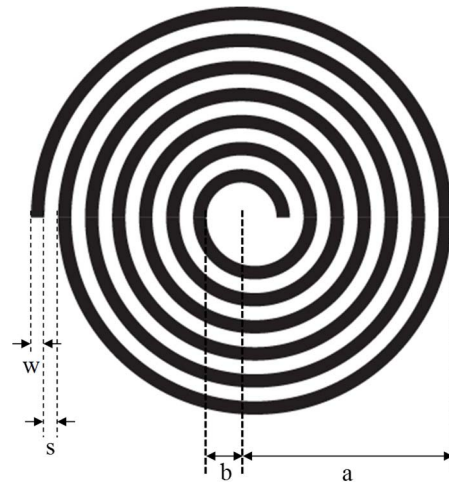


Fig. 1. Top view of the resonator for WPT.

circular coil antenna needs a winding machine, which has high design accuracy. The winding machine should be reengineered when the coil antenna is changed. Because of this reason, the print-based antenna is researched [1]. The printed-based antenna (see Fig. 2) has some advantages compared with the circular coil antenna. First, it has high productivity. Thus, it is very advantageous for mass production. Second, it is so thin that it can be applied to any application. However, the printed-based antenna is too thin to satisfy the skin depth, so it has higher resistance than the conventional antenna. This eventually leads to a low quality factor ( $Q$ -factor) and low transmission efficiency. This article investigates the parasitic components generated in the antenna to improve the low  $Q$ -factor of the print-based antenna. To increase Tx coil to Rx coil transmission efficiency, the coupling coefficient should be increased. Also, the  $Q$ -factor of each antenna should be increased, as shown in (1) [1].

In order to explain how the  $Q$ -factor affects the efficiency in the wireless power transmission system, the transmission efficiency is calculated through the equivalent circuit (see Fig. 3) of the wireless power transmission system, and then, the transmission efficiency is expressed as (3). In (3), it can be seen that the higher the  $Q$ -factor of the transmitting and receiving antenna, the higher the transmission efficiency.

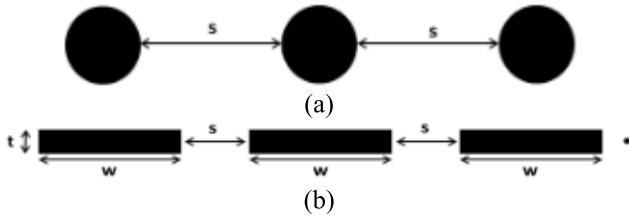


Fig. 2. Cross-sectional diagram of (a) circular coil antenna and (b) print-based antenna.

TABLE I  
DESIGN CONSTRAINTS

Symbol	Quantity	Value
$f$	Frequency	6.78Mhz
$t_c$	Copper thickness	35um
$h$	Substrate thickness	200um
$m$	Magnetic permeability	1.256uH/m
$p$	Conductivity	16.7nΩ*m
$\Delta$	Skin depth	25um
$a$	Outer radius	Variable
$n$	Turn number	2
$w$	Width	Variable
$s$	Pitch	Variable
$w + s$	Width + Pitch	6mm

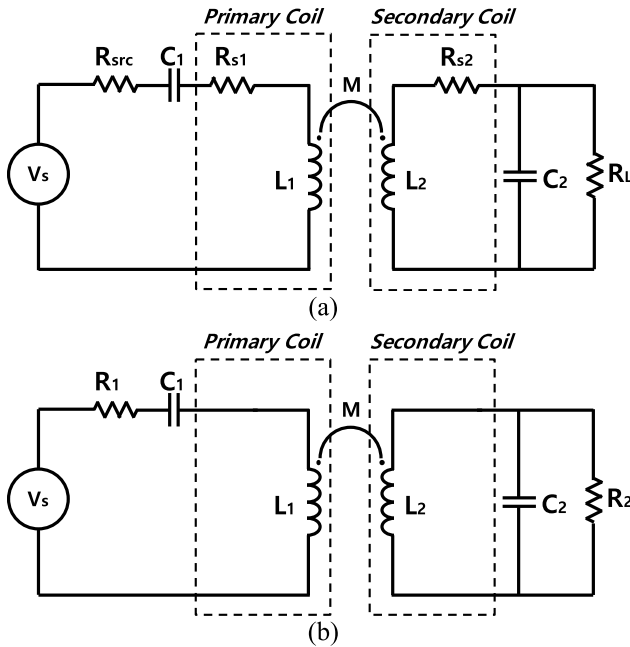


Fig. 3. (a) Original schematic for inductive coupled. (b) Parallel-to-series approximated schematic [1].

inner diameter, are fixed. However, if all the parameters have variable values, the results of [2] and [3] are not accurate. This article proposes a method to achieve the high  $Q$ -factor in any condition. The inaccuracy of [2] and [3] is caused by the difficulty of modeling. Thus, this article is not focused on accurate modeling but concentrated on a tendency about how these parameters influence the  $Q$ -factor. Also, based on this tendency, a new structure for the high  $Q$ -factor is proposed. In the past, research for a high  $Q$ -factor of the printed resonator has been conducted [4], [5]. However, in this article, the relationship between the parasitic component of the resonator and the form factors that make up the resonator was also investigated.

Equations (1) and (2) are used to approximate a general equivalent circuit for ease of calculation. The description of this approach is well explained in [1], so we will not elaborate on it in this article

$$R_1 = R_{src} + R_{s1} \tag{1}$$

$$R_2 = R_L || R_{p2} \tag{2}$$

$$\eta_{max} = \frac{1}{1 + 1/(k^2 Q_1 Q_2)} \frac{R_{p2}}{R_{p2} + R_L} \tag{3}$$

where  $R_{p2}$  is the approximated resistance of  $R_{s2}$  and  $R_L$  is the load resistance.  $Q_1$  and  $Q_2$  are  $Q$ -factors of each antenna. In the print-based antenna, there are many parameters, such as linewidth and pitch, the number of turns, and outer and inner diameters. It is hard to do modeling precisely because these parameters are dependent on each other. Thus, existing papers have different opinions about the parameters. One says that the  $Q$ -factor becomes the highest when the line pitch becomes the largest [2]. The other says that the  $Q$ -factor can have the highest value when pitch and width have a 2:1 ratio without any influence of diameter [3]. Both of them are accurate in specific conditions. The specific condition means the case that some parameters, such as outer diameter or

Considering the user charging convenience aspect, the greater the separation distance between the transmitting and receiving antennas, the higher the degree of freedom of charging (convenience) in the space. In order to provide the efficiency and stability of charging compared to the existing magnetic induction method, the transmission/reception distance has been extended. In this article, the transmission distance was set to achieve the maximum transmission efficiency at the size of a smartphone, and as a result, it was found that the maximum transmission efficiency appeared at a distance of about 1.5–2 cm. In addition, in this article, the relationship between the form factor of the resonator and the transmission distance is investigated, and a method of designing to have the maximum efficiency at the desired transmission distance is introduced.

In addition to the  $Q$ -factor, the coupling correlation factor is also related to efficiency. The coupling coefficient determines the distance at which critical coupling occurs and how to control it is briefly mentioned in Section IV-B. The coupling coefficient is most closely related to the mutual inductance between the transmitting and receiving antennas. In this article, the resonance performance that a single antenna can have is mainly discussed.

In Section II, mathematical modeling of the print-based antenna is performed by a commercial programming tool. In Section III, the result of modeling is analyzed. Finally, a new structure based on the result is proposed and compared with the existing structure by making the experimental prototype.

## II. MODELING OF RESONATOR PARASITIC COMPONENTS

Parameters of the print-based antenna are set, as shown in Figs. 1 and 2.  $w$ ,  $s$ ,  $a$ , and  $b$  mean linewidth, pitch, outer radius, and inner radius, and  $t$  means thickness. Other parameters are set, as shown in Table I. The  $Q$ -factor can be calculated if inductance and resistance are known because the  $Q$ -factor is calculated by

$$Q = \frac{\omega L}{R}. \quad (4)$$

By this equation, we can know that the resistance should have a low value and the inductance should have a high value to achieve a high  $Q$ -factor. The inductance and resistance can be obtained in the following.

### A. Inductance

There are two types of inductance. One is series inductance, and the other is mutual inductance between adjacent two lines. The series inductance is the major factor of coil antenna. It can be mathematically expressed as [1]

$$L_s = \frac{1.27\mu_0 n^2 d_{\text{avg}}}{2} \left[ \ln\left(\frac{2.07}{\varphi}\right) + 0.18\varphi + 0.13\varphi^2 \right] \quad (5)$$

$$\varphi = \frac{d_o - d_i}{d_o + d_i} \quad (6)$$

where  $d_o$  and  $d_i$  are the outer and inner diameters of the antenna, and  $d_{\text{avg}} = (d_o + d_i)/2$ .  $n$  means the number of turns. Through this equation, we can see that the series inductance is directly proportional to outer, inner diameters, and turn number. It seems like that the outer and inner diameters or turn numbers are unrelated things. However, the parameters are connected by one parameter, line length. If the outer diameter is increased, the line length would be also increased when other parameters are fixed. The inner diameter and turn number are also directly proportional to line length. Consequently, the series inductance is directly proportional to line length.

The mutual inductance of adjacent two lines in a single coil (see Fig. 4) can be expressed as Neumann's formula

$$L_M = \frac{\mu_0}{4\pi} \oint_{C_2} \oint_{C_1} \frac{dl_1 \cdot dl_2}{|\vec{R}|}. \quad (7)$$

By this equation, it can be found that the mutual inductance is inversely proportional to pitch between adjacent lines because  $|\vec{R}|$  is directly proportional to outer diameter because of  $dl_1 \cdot dl_2$ .

### B. Resistance

There are two kinds of resistance that we should be considered: the first is skin effect resistance, and the second is proximity effect resistance. There are also other resistances, such as radiation loss or core loss. However, the radiation loss is too small to consider, and also, there is no core loss because we use an air core. Finally, there is a substrate loss, but this is also a very small value, which is negligible [6]. Thus, the skin and proximity resistance take the most of the part of total resistance.

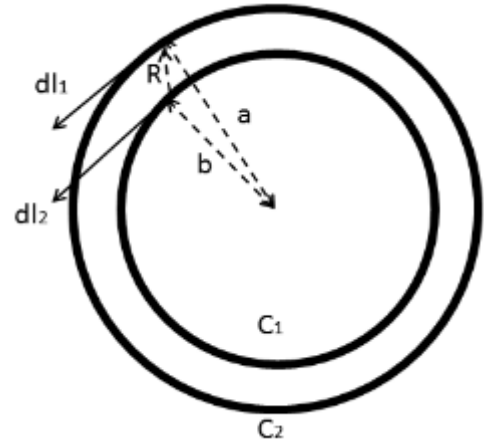


Fig. 4. Top view of the two-turn antenna for mutual inductance.

The effective series resistance is comprised of skin and proximity resistance as stated above. It can be calculated by [2]

$$R = R_{\text{dc}} \left( 1 + \frac{1}{1 - A'/A} + \frac{1}{10} \left( \frac{\omega}{\omega_{\text{crit}}} \right)^2 \right) \quad (8)$$

$$\omega_{\text{crit}} = \frac{3.1 \cdot (w + s) \cdot \rho}{\mu \cdot w^2 \cdot t}. \quad (9)$$

Equation (8) can be divided into three parts,  $R_{\text{dc}}$ ,  $R_{\text{dc}} \cdot 1/(1 - (A'/A))$ , and  $(R_{\text{dc}}/10) \cdot (\omega/(\omega_{\text{crit}}))^2$ . In these three parts, the second part means the skin effect resistance,  $R_s$ .  $A$  means the cross-sectional area.  $A'$  that means an effective area reduction can be expressed as

$$A' = (w - 2\delta)(t - 2\delta). \quad (10)$$

Through this skin resistance is closely related with the linewidth, the result is shown in Fig. 5. The third part of effective series resistance means the proximity resistance,  $R_p$ . We can find that this parameter is also related to the linewidth. Also, the pitch is related to this. The result is indicated in Fig. 5.

### C. Capacitance

According to [7], there are two types of materials affecting this capacitance: one is air and the other is the substrate. Therefore, the total capacitance  $C_P$  can be divided into  $C_{Pc}$  and  $C_{Ps}$  components

$$C_P = C_{Pc} + C_{Ps} \approx (a\varepsilon_{\text{rc}} + \beta\varepsilon_{\text{rs}})\varepsilon_0 \frac{t_c}{s} l_g$$

where  $\varepsilon_{\text{rc}}$  and  $\varepsilon_{\text{rs}}$  are the relative dielectric constants of the air and substrate materials, respectively. According to [7],  $(\alpha, \beta) = (0.9, 0.1)$  can be found empirically for air and FR4. From insulator characteristic tables,  $(\varepsilon_{\text{rc}}, \varepsilon_{\text{rs}}) = (1, 4.4)$ .  $l_g$  is the total length of the gap, and it can be calculated as

$$l_g = 4(d_o - w \cdot n)(n - 1) - 4s \cdot n(n + 1).$$

The parasitic capacitance can be obtained through the above equation, but the thickness of the printed base resonator is very thin, so the parasitic capacitance is very small. Since the

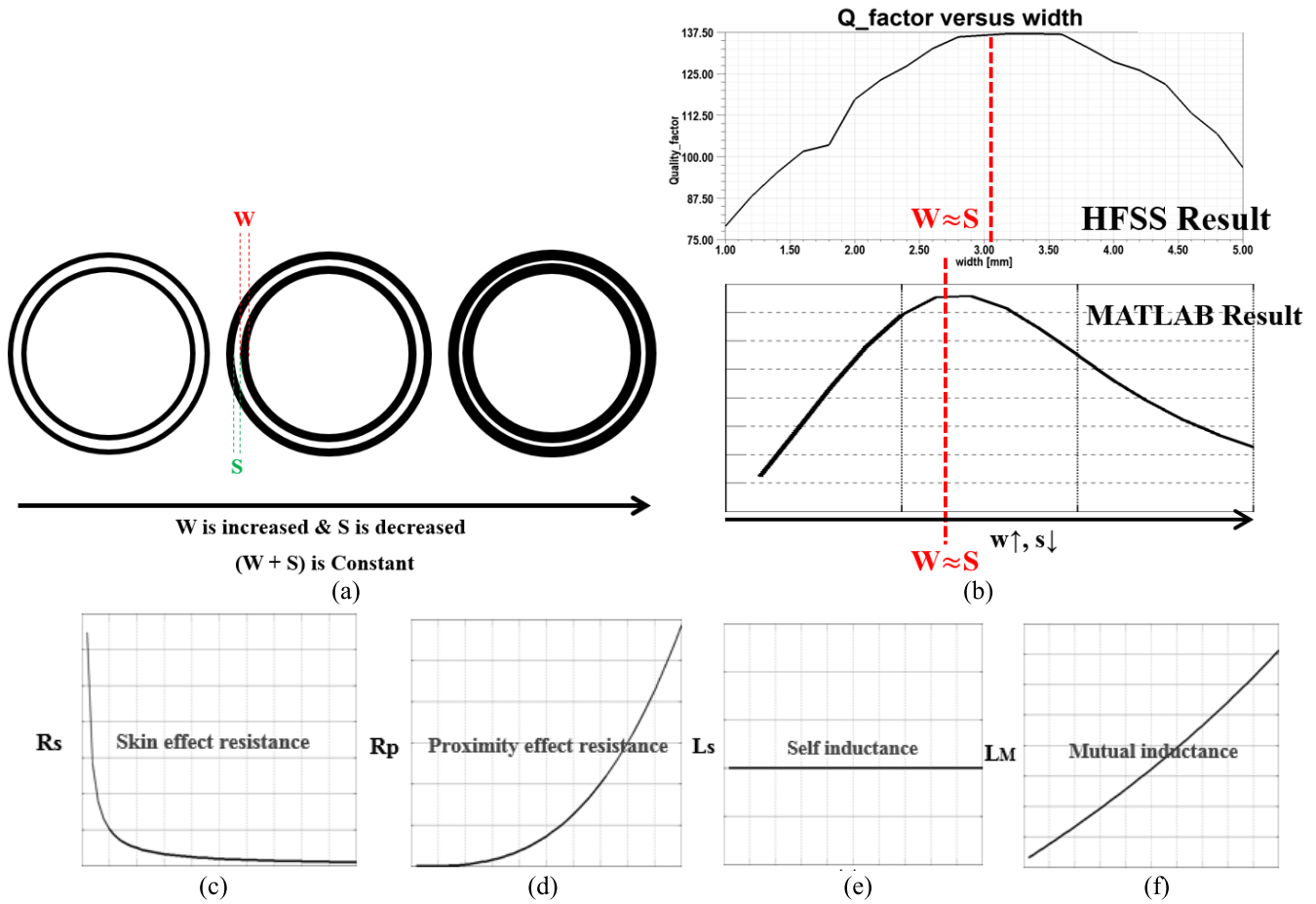


Fig. 5. Parasitic component of the printed base antenna according to (a) change of width and pitch, (b)  $Q$ -factor simulated using commercial 3-D analysis tool and commercial programming tool, (c) skin effect resistance, (d) proximity effect resistance, (e) self-inductance, and (f) mutual inductance simulated using a commercial programming tool.

parasitic capacitance of the printed base resonator does not affect the  $Q$ -factor, it is ignored in this article.

### III. ANALYSIS OF THE RELATIONSHIP BETWEEN THE QUALITY FACTOR AND EACH VARIABLE THAT DETERMINES THE FORM FACTOR

#### A. Relationship Between Quality-Factor and Width & Pitch

The relationship between parameters and  $Q$ -factor can be inferred through modeling results. Since the parameters are connected to each other, we have to separate them. To isolate the parameters each other,  $(w + s)$  should have a fixed value. Because if  $w$  or  $s$  is an independent variable, all the parameters, such as turn number, and outer and inner diameters, can be changed as  $w$  or  $s$  has changed. Thus, by changing solely the ratio of  $w$  &  $s$ , the turn number or other parameter can be stabilized; after that, the resistance and inductance can be checked with changing ratio of  $w$  &  $s$  without any influence of other parameters. The result is indicated in Fig. 5.

Skin effect resistance and proximity effect resistance are variables affected by width and pitch, respectively. That is, as the width increases, the area of the cross section increases, and the skin effect resistance decreases. Also, as the pitch decreases, the coupling coefficient between two

adjacent lines increases, and the proximity effect resistance increases. The mutual inductance is increased with decreasing pitch because of Neumann's formula. However, the series inductance has not any variation with changing width and pitch because it is related to the line length as stated above. Consequently, the indicator of the  $Q$ -factor has the maximum value at a specific point, as shown in Fig. 5. This means that  $w$  &  $s$  have a specific ratio to make the  $Q$ -factor maximum. We can confirm that the ratio is 1:1 through Figs. 5 and 6.

When we made a real resonator, we could get the result, as shown in Fig. 6. In the case of resistance, since it is the sum of skin effect resistance and proximity effect resistance, it tends to decrease and then increase as the ratio of width and pitch changes as expected. In the case of inductance, since it is the sum of self-inductance and mutual inductance, it was expected to show an increasing trend, but the actual size of mutual inductance itself was very small compared to self-inductance, and the effect was negligible. Rather, it showed a tendency to slightly decrease due to the parasitic capacitance that occurs as the two lines get closer. As a result, when the width and pitch were the same value, the largest  $Q$ -factor was shown, and the difference was about two times compared to the smallest value.

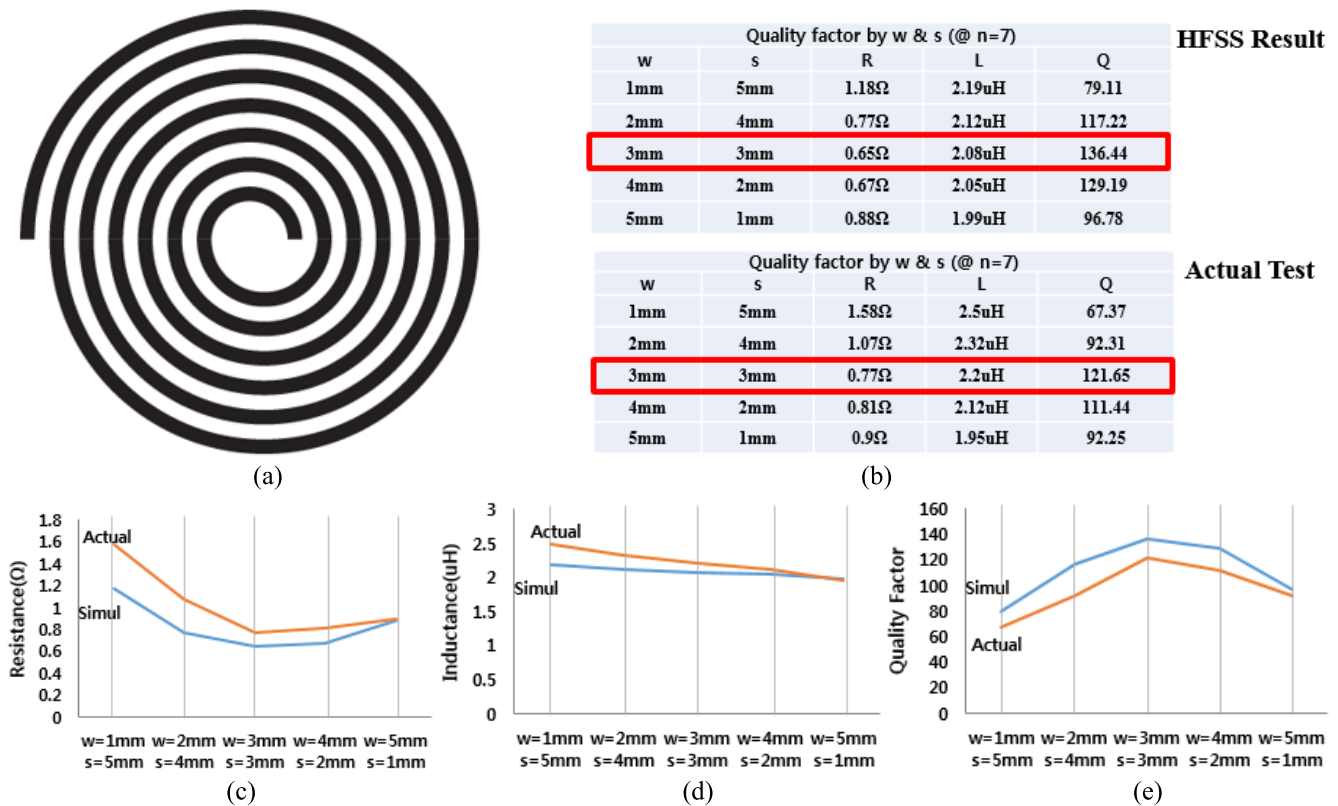


Fig. 6. (a) Top view of conventional type resonator. (b) Comparison of results using commercial simulation tools and actual test results. Graphs of (c) resistance, (d) inductance, and (e)  $Q$ -factor.

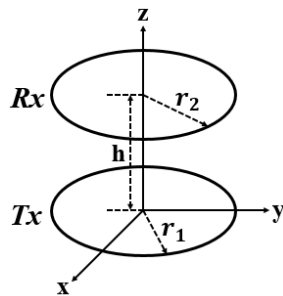


Fig. 7. Model to explain Neumann's formula.

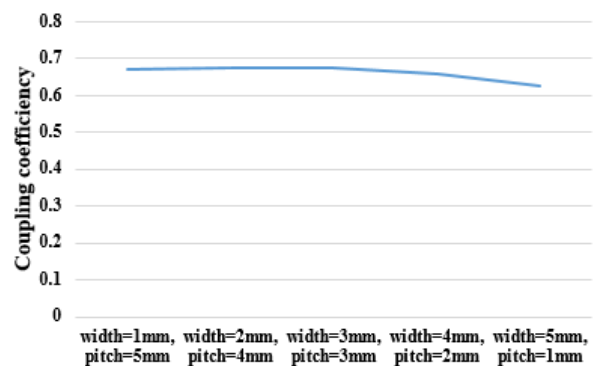


Fig. 8. Coupling coefficient according to width and pitch length.

When performing the printed antenna manufacturing process, not only the copper is cut but also the pr coating is cut during the etching process, so the width of the line may be thinner than the design value. As a result, the cross-sectional area is reduced, and the skin effect resistance may be slightly larger than that of the simulation. In the case of inductance, the width decreases, the gap between the lines increases, and the influence of mutual inductance decreases. Eventually, compared to simulation, a little higher inductance is formed. Since the degree of etching is the same, when the width is narrow, as shown in Fig. 6, there is more difference from simulation.

From the above results, it can be seen that maximizing the  $Q$ -factor by adjusting the width and pitch is not related to the coupling factor. The coupling coefficient formula is

$k = M/(L_1 L_2)^{1/2}$ . That is, when transmitting and receiving resonators are present (see Fig. 7), the inductance of each resonator and the mutual inductance between the two antennas determine the coupling coefficient. In this article, a method for maximizing the  $Q$ -factor by adjusting the linewidth and line-to-line distance of a single resonator is presented. According to the experimental results (see Fig. 6), it can be confirmed that the inductance does not change significantly even if the linewidth and the line distance of the resonator are adjusted, and only the resistance changes significantly.

Also, according to the Neumann formula shown in (7), the mutual inductance is determined by the distance between the transmitting and receiving resonators. The distance of

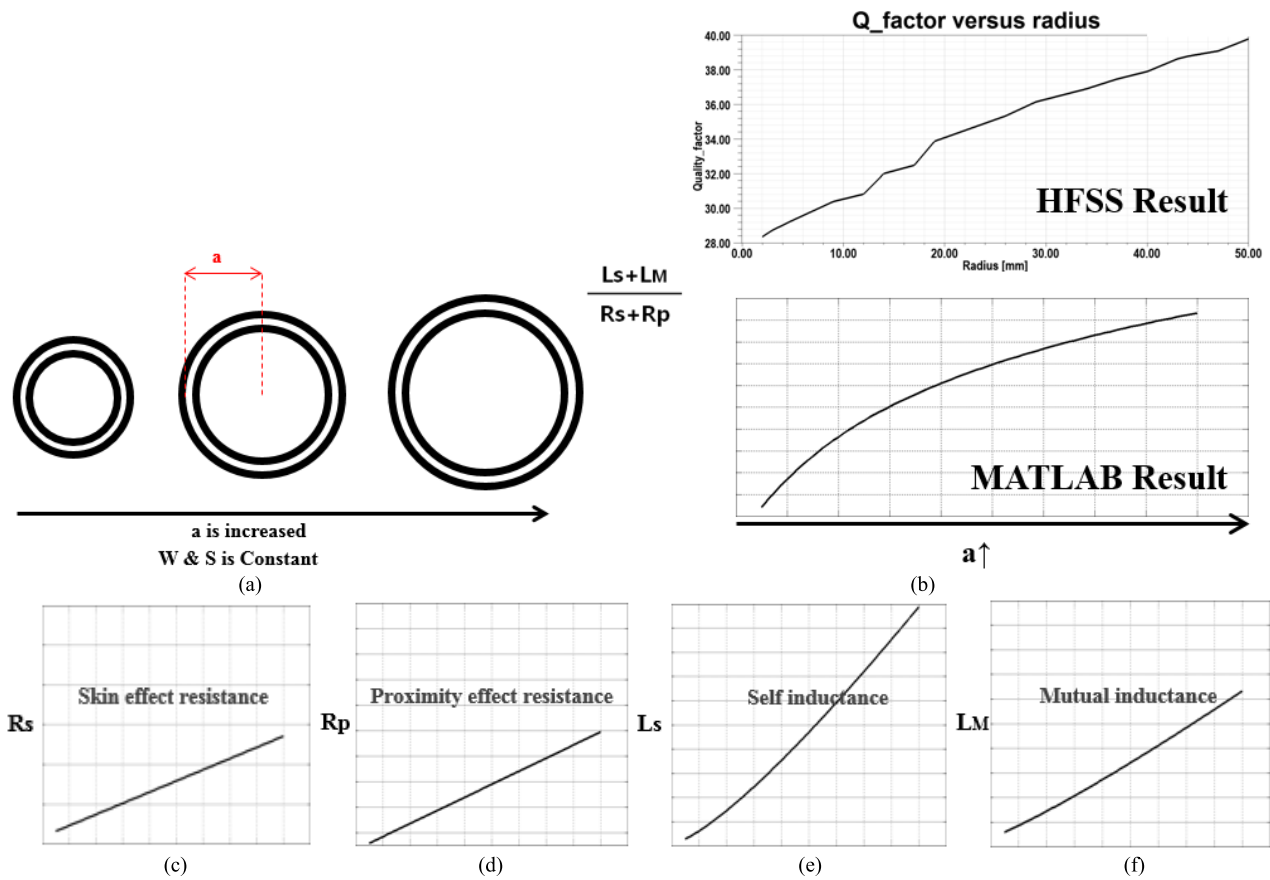


Fig. 9. Parasitic component of the printed base antenna according to (a) change of radius, (b) *Q*-factor simulated using commercial 3-D analysis tool and commercial programming tool, (c) skin effect resistance, (d) proximity effect resistance, (e) self-inductance, and (f) mutual inductance simulated using a commercial programming tool.

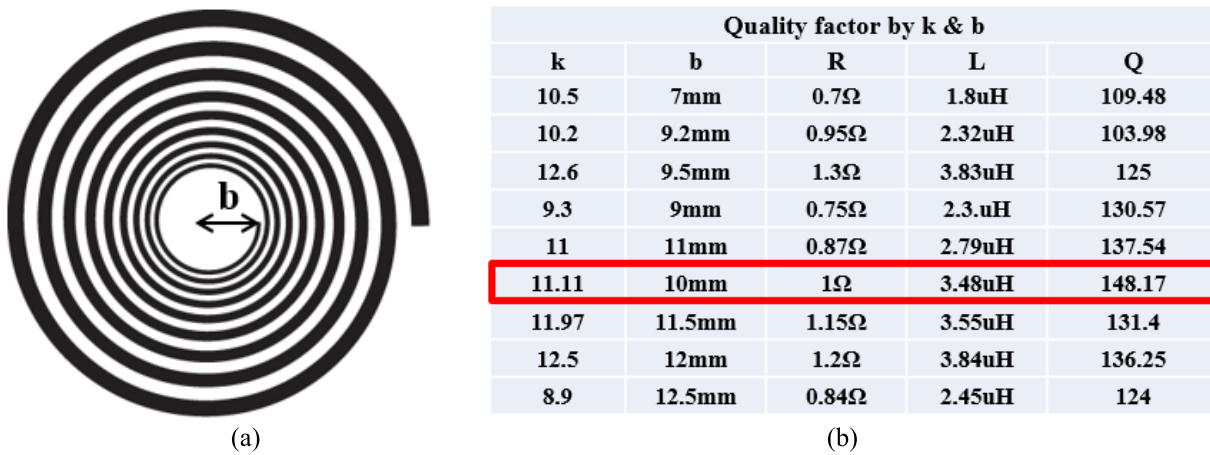


Fig. 10. (a) Top view of the unequal antenna and (b) its parasitic component.

the transceiver resonator can be divided into a horizontal distance ( $r_2-r_1$ ) and a vertical distance ( $h$ ). The horizontal distance is determined by the difference in the radius of the transmitting and receiving resonators, and the vertical distance is the distance between the resonators. However, in this article, the *Q*-factor was maximized by adjusting only the linewidth and the line distance while maintaining the radius. Therefore, based on the above two reasons, it can be seen that the method of improving the *Q*-factor presented in this article is not significantly related to the coupling factor. Fig. 8 shows the result. It can be seen that the coupling coefficient is maintained

almost constant when the simulation is performed by changing the width and pitch on a commercial 3-D analysis tool.

*B. Relationship Between Quality-Factor and Diameter*

In this variable, other parameters also need to be stabilized. For the convenience of analysis, the turn number is set as 2. After that, the resistance and inductance are checked by changing the diameter.

All the figures are rescaled on the same scale to compare a slope easily. We can see that the slope of series inductance

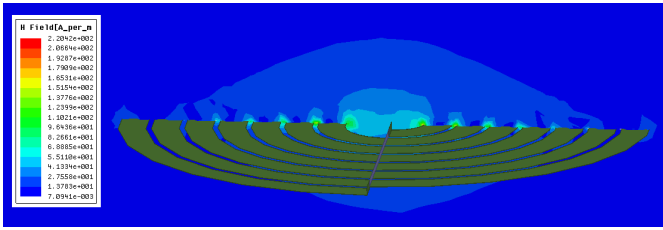


Fig. 11.  $H$ -field distribution of the printed base antenna (6.78 MHz and 1 W).

is the steepest. The series inductance is increased rapidly than resistance when the diameter is increased. This means that the  $Q$ -factor has a possibility to be higher when the diameter of the antenna is increased. Fig. 9 supports this fact.

### C. Proposed Antenna

Based on all the results, the new structure antenna is proposed, as shown in Fig. 10. This figure has a structure that width and pitch are increased as the diameter is increased because Section III-B teaches us that the  $Q$ -factor can be increased when the diameter is increased. In fact, as shown in Fig. 11, the  $H$ -field is a structure that is heavily concentrated in the center of the resonator. This means that the centerline is more vulnerable to the proximity effect, so it is advantageous to design the centerline to be thin and the outer line to be thick. In summary, there are skin effect resistance and proximity effect resistance in the resistance component. Since the  $H$ -field is concentrated in the center of the resonator, the proximity effect resistance can increase. Therefore, if the centerline is designed to be thin, and the more it is off the center, the thicker it is to minimize proximity effect resistance. In the end, the structure of the unequal resonator, as shown in Fig. 10, can help to improve the  $Q$ -factor.

A constant is presented to mathematically express the antenna easily. With this constant, the proposed antenna can be expressed by just two parameters. When we call the distance between the center and some lines as  $d$ , the linewidth can be expressed as

$$d = k * w. \quad (11)$$

From the above results, we found that the best  $Q$ -factor can be obtained when the ratio of width and pitch is 1:1. Based on this result and the fact that, as the radius of the antenna increases, the  $Q$ -factor increases, we have devised a new structure and proposed a variable  $k$  to simply represent the structure. In short, the new antennas are structured by three facts:

- 1) innermost diameter “ $b$ ”;
- 2) unequal factor “ $k$ ”;
- 3) ratio of width and pitch “1:1.”

Of these three, we have to determine the inner diameters  $b$  and  $k$  of the antenna. As stated above, the new antenna can be mathematically expressed with a new constant  $k$  and inner diameter  $b$ .  $k$  is a ratio between  $w$  and  $d$ . Some test is performed with the parameters. With Fig. 10, we can see

that the  $Q$ -factor has the highest value when  $k = 11.11$  and  $b = 10$  mm. In this case, the  $Q$ -factor of the proposed antenna is higher than the conventional type almost 21.8%. Generally, the  $Q$ -factor has a high value at  $k \approx b$ .

Fig. 12 shows the  $Q$ -factor according to the innermost radius “ $b$ ” and the unequal factor “ $k$ ” obtained using a commercial simulation tool. It can be seen from the figure that it shows the maximum  $Q$ -factor ( $Q_{\text{factor}} = 149$ ) under conditions similar to the experimental results ( $k = 11$  and  $b = 11$ ). Also, it can be seen that the unequal factor has a greater influence on the  $Q$ -factor than the innermost radius through this experimental result. In other words, the linewidth ( $w$ ) and the line distance ( $s$ ) are strongly related to the  $Q$ -factor, and it can be seen that minimizing the aforementioned two types of resistance (skin and proximity) is the most important to maximize the  $Q$ -factor.

Finally, it can be seen that, when the distance is changed, as shown in Fig. 13, the coupling coefficient also changes significantly. At this time, the difference from the existing resonator was not significant. In the case of the unequal resonator, the inductance increases as the turn number increases, but, since the mutual inductance also increases, it can be seen that the coupling coefficient is not significantly affected.

In this article, we describe how to set up important initial variables in resonator design before optimization and to determine each variable. Fig. 14 shows the unequal resonator design process presented in this article. The design was carried out in such a way that the form factors constituting each resonator were listed and variables were removed while deciding one by one.

First, we tried to understand the relationship between the form factor constituting the existing resonator and the electrical parasitic components. Through this, it was possible to confirm which parasitic components have a great influence in designing the resonator, as well as to suggest the conditions for maximizing the  $Q$ -factor. As can be seen in Fig. 14, an unequal resonator was proposed through the previous results, and “ $k$ ,” a parameter that can define the unequal resonator, was presented. Finally, through finite element simulation with innermost radius “ $b$ ,” the value that can maximize the  $Q$ -factor was confirmed.

## IV. WIRELESS POWER TRANSMISSION TEST

### A. Efficiency Test

S21 of the two antennas presented in Fig. 15(b) and (c) is measured, as shown in Fig. 15(a). We use a general Tx antenna to compare the antennas accurately. As a result, S21 of the conventional antenna is  $-2.3793$  dB, and S21 of the new antenna is  $-1.6760$  dB at 4 cm. It means that the efficiency of the new antenna is higher than the efficiency of the conventional antenna about 10%, as shown in Fig. 16. If we use a pair of the new antenna, the efficiency gap will be more severe. Overall, the efficiency of the new antenna is improved at under coupling area. The efficiency is low at over coupling area. However, over coupling can be overcome by adaptive impedance matching. From this result, it can be

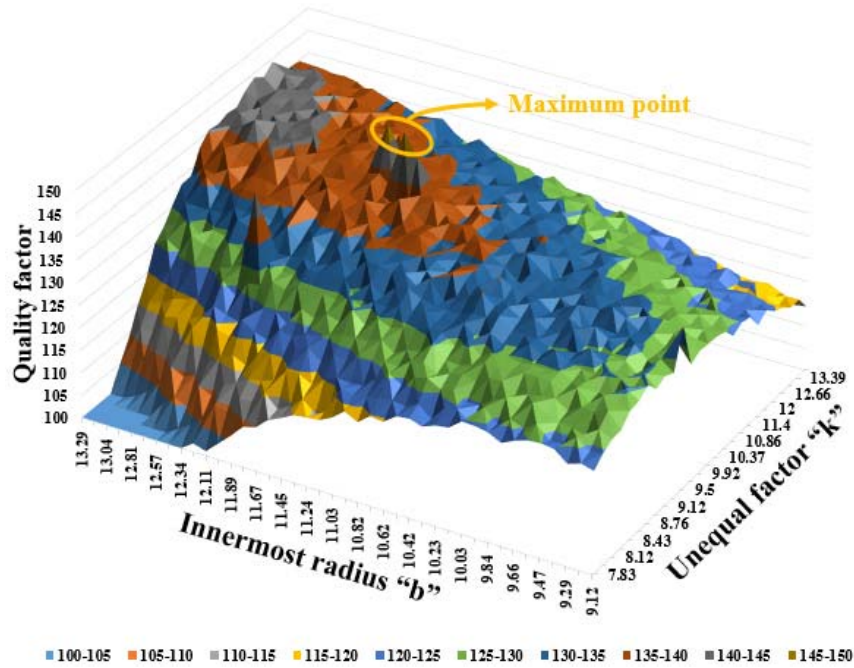


Fig. 12. Q-factor simulation result according to the innermost radius and unequal factor.

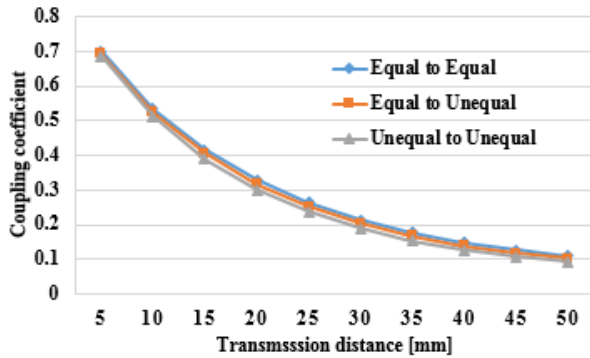


Fig. 13. Coupling coefficient according to power transmission distance.

confirmed that power transmission efficiency can be improved through an unequal structure with a high Q-factor.

**B. Comparison With Conventional Coil Antenna**

In this section, we compare the proposed printed antenna with the conventional antenna. For the conventional coil antenna, the thickness and the outer diameter are made the same as the printed antenna, and the “unequal pitch” is applied for the best Q-factor. All resonators were manufactured using SS resonant coupling. The result is shown as follows.

Fig. 17(a)–(c) lists the antennas manufactured using common coils. They are named c1, c2, and c3, respectively, and their characteristics are shown in Table II. The parameter resistance (R) and inductance (L) were measured through a network analyzer (E5071A), and Q was calculated through the measured R and L. In Table II, c3 with unequal pitch showed the highest Q-factor. Also, Fig. 17(d)–(f) shows the basic form antenna, antenna with unequal pitch only, and antenna with

TABLE II  
FIG. 17(a)–(f): ANTENNA TEST RESULT (ACTUAL MEASUREMENT)

Type	R	L	Q
c1	4.6Ω	11.6uH	107.37
c2	18.7Ω	44uH	100.18
c3	6.4Ω	17uH	113
p1	0.77Ω	2.2uH	121.65
p2	0.67Ω	2.16uH	137.26
p3	1Ω	3.48uH	148.17

TABLE III  
FIG. 13(a)–(c): ANTENNA TEST RESULT (ACTUAL MEASUREMENT)

Type	R	L	Q
t1	3.1Ω	10.8uH	143.7
t2	12Ω	15.8uH	56.06
t3	47Ω	35uH	31.7

TABLE IV  
FIG. 18(a)–(d): ANTENNA TEST RESULT (ACTUAL MEASUREMENT)

Type	R	L	Q
t1	3.1Ω	10.8uH	148.3
t2	12Ω	15.8uH	56.06
t3	47Ω	35uH	31.7
p4	3Ω	9.3uH	132

both unequal pitch and unequal width, and their characteristics are shown in Table II. The results show that the antenna with unequal pitch and unequal width has the highest Q-factor. From these results, we can see that the proposed printed

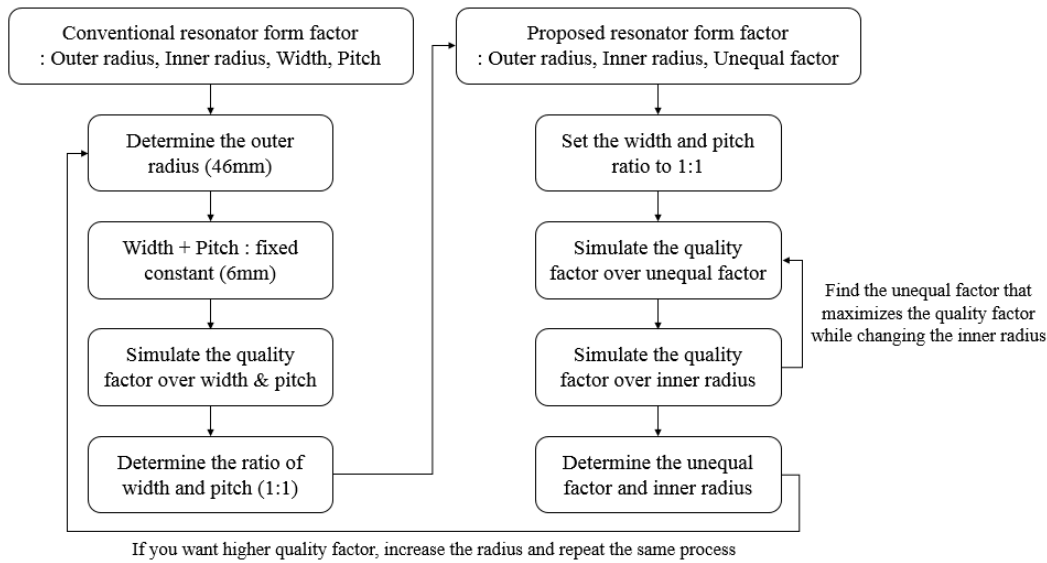


Fig. 14. Proposed unequal resonator design process.

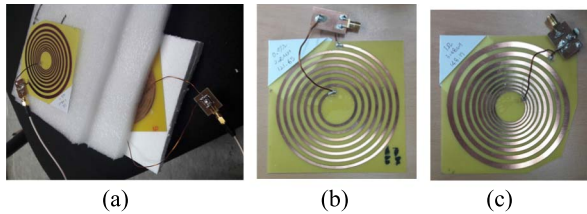


Fig. 15. (a) Test bed using Styrofoam to minimize external influence. (b) Equal printed-based antenna. (c) Unequal printed base antenna.

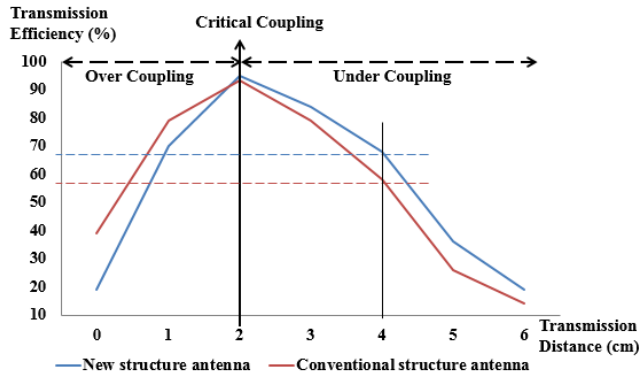


Fig. 16. Wireless power transmission efficiency to show the performance improvement of the proposed antenna.

antenna guarantees a higher  $Q$ -factor than the conventional antenna in the same condition. However, it can be seen that the inductance of the conventional antenna is relatively higher than that of the printed antenna. In general, the inductance is related to the transmission distance, and the  $Q$ -factor is related to the transmission efficiency. In order to compare these characteristics, an antenna with a size of 23 cm  $\times$  14 cm was fabricated, and the experiment was conducted.

First, Fig. 18 shows the transmit antennas that are fabricated, and their characteristics are shown in Table III. As with the

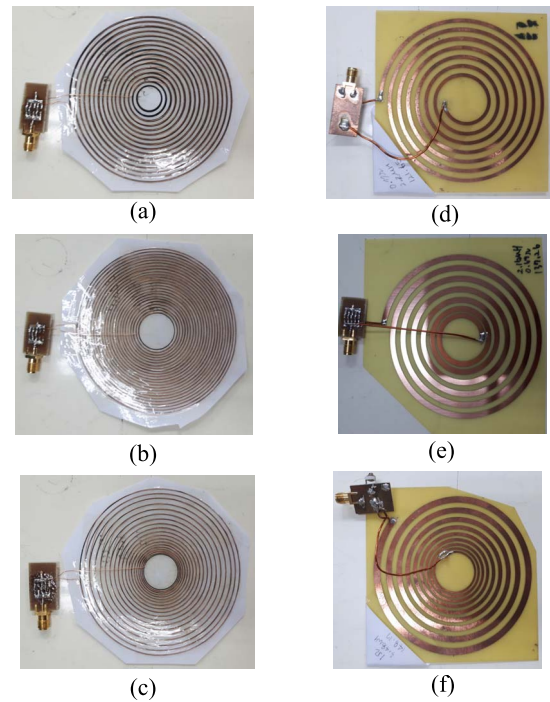


Fig. 17. (a) Coil antenna (turn number: 14 and pitch: 4 mm) (Rx\_coil1). (b) Coil antenna (turn number: 23 and pitch: 1.5 mm) (Rx\_coil2). (c) Coil antenna (turn number: 18 and pitch: unequal) (Rx\_coil3). (d) Printed antenna (turn number: 7 and pitch: 3 mm) (Rx\_print1). (e) Printed antenna (turn number: 6 and pitch: unequal) (Rx\_print2). (f) Printed antenna (turn number: 9 and pitch: unequal) (Rx\_print3).

previous results, the  $Q$ -factor of the proposed antenna is high. However, the inductance was higher in the coil antenna than before. The power transmission experiments were performed using these transmit antennas according to the following procedure (see Fig. 19):

- 1) First, generate a 6.78-MHz signal from the signal generator.

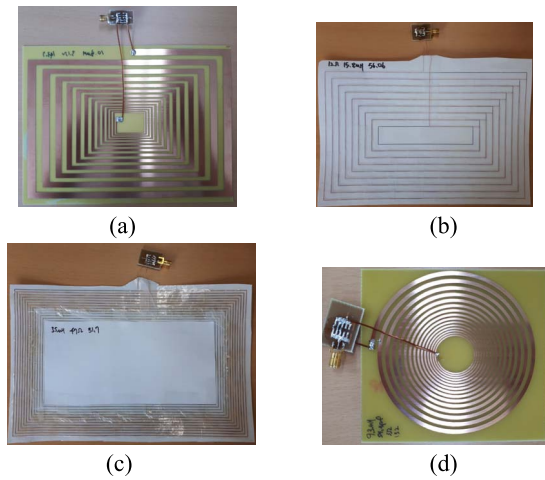


Fig. 18. (a) Printed antenna (turn number: 13 and pitch: unequal) (Tx1). (b) Coil antenna (turn number: 8 and pitch: 7.5 mm) (Tx2). (c) Coil antenna (turn number: 8 and pitch: 2.5 mm) (Tx3). (d) Printed antenna (turn number: 15 and pitch: unequal) (Rx\_print4).

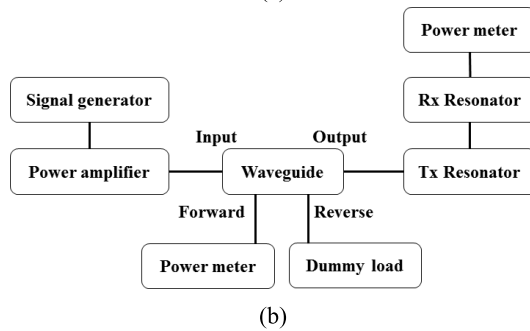
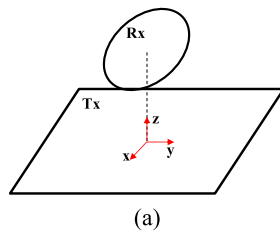


Fig. 19. (a) Experiment environment. A rectangular antenna ( $t1$ ,  $t2$ , and  $t2$ ) was used as a transmission (Tx) antenna, and a circular antenna ( $c1$ ,  $c2$ ,  $c3$ ,  $p1$ ,  $p2$ , and  $p3$ ) was used as a receiving (Rx) antenna. (b) Block diagram of how to measure remission efficiency.

- 2) Amplify the generated signal to the desired power level (1 W) through a power amplifier.
- 3) Since the impedance of the resonator can change according to the coupling coefficient, the power is transferred to the resonator through the waveguide, and the output of the amplifier is determined by reading the forward power of the waveguide.
- 4) The power delivered to the Tx resonator is wirelessly delivered to the Rx resonator, and the power at this time is read by a power meter.
- 5) Transmission efficiency can be read through the values of two power meters.

The results are shown in Fig. 20. As can be seen in Fig. 20, the transmission efficiency at critical coupling was higher

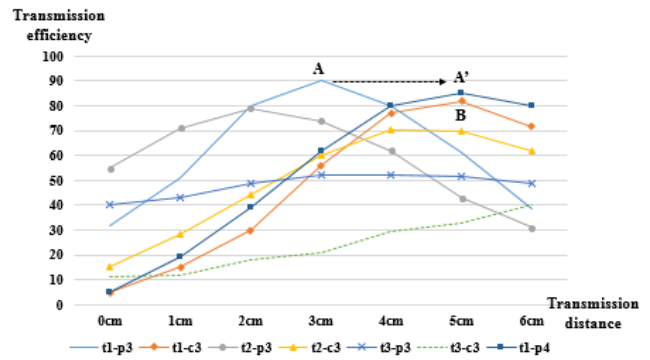


Fig. 20. Comparison of transmit efficiency according to the  $z$ -axis change.

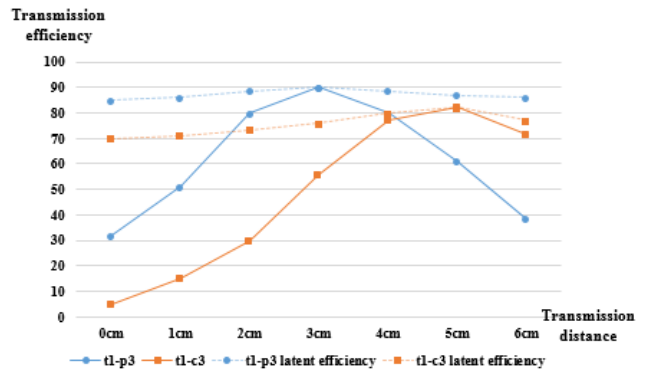


Fig. 21. Comparison of transmit latent efficiency according to the  $z$ -axis change.

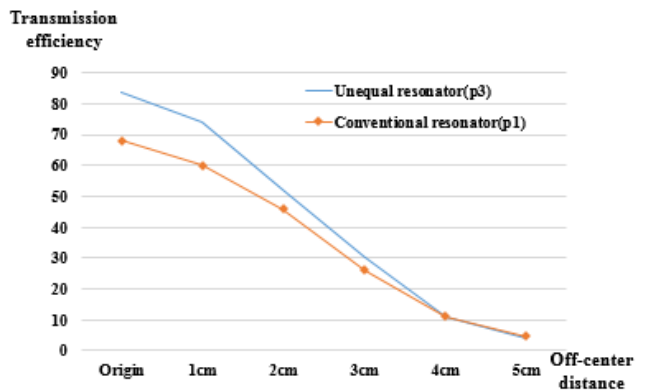


Fig. 22. Comparison of transmit efficiency according to  $x$ - and  $y$ -axis changes.

for the printed antenna (point A) than for the coil antenna (point B). However, the coil antenna of which the inductance value was high was excellent in the transmission distance. However, it is not impossible to increase the distance if the printed antenna abandons the high  $Q$ -factor. That is, it is possible to move the critical coupling point from point A to point B. To illustrate this, another printed antenna (Rx\_print4) was fabricated. The antenna (Rx\_print4) in Fig. 18 is an antenna fabricated using unequal pitch and unequal width techniques. The difference is to extend the maximum distance, give up the  $Q$ -factor, and increase the inductance. In summary,

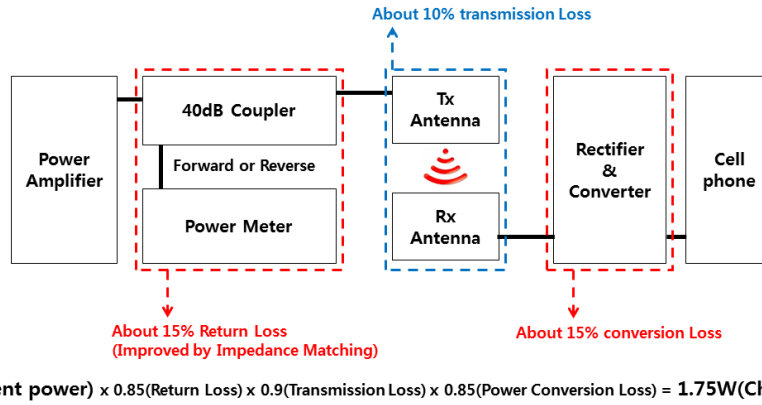


Fig. 23. Cell phone charging experiment block diagram and distribution of losses.

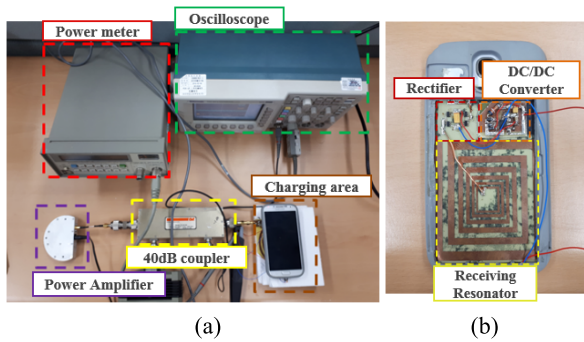


Fig. 24. (a) Cell phone charging testbed. (b) Receiving part.

since securing the best efficiency and maximum transmission distance is important when designing a resonator, in this article, we first find the point where the efficiency is the best by maximizing the  $Q$ -factor (point A), and second, by adjusting the inductance value, a wider transmission distance (point A') was achieved.

In Fig. 20, it is seen that the maximum efficiency is somewhat reduced because the  $Q$ -factor is decreased, but the transmission distance is the same as that of the coil antenna (Rx\_coil3), and the efficiency is higher than the coil antenna. The critical coupling point of the Rx\_print4 resonator was called A'. In this way, the printed antenna has the advantage that it can be freely designed according to the design purpose. On the other hand, in the case of a coil antenna, the critical coupling point can be shifted from point B to point A, but it is difficult to ensure high efficiency compared to a printed antenna. The contents shown in Fig. 21 show the maximum point of the antenna by designing the antenna that can maximize the efficiency at each distance by adjusting the inductance of the antenna. As can be seen from the graph, the unequal design method can design an antenna with higher efficiency than the conventional coil antenna.

Fig. 22 shows a comparison of the power transmission efficiency of the conventional antenna and the proposed antenna when the receiving resonator is moved to the  $x$ -axis or the  $y$ -axis instead of the  $z$ -axis. An Rx\_print1 resonator was used as a transmit antenna, and an Rx\_print1 resonator and an Rx\_print3 resonator were used as the receiving antenna.

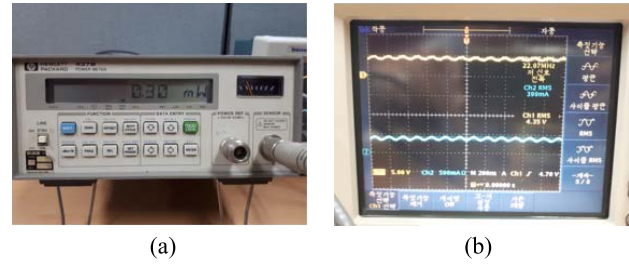


Fig. 25. (a) Power meter measurement result. (b) Oscilloscope measurement result.

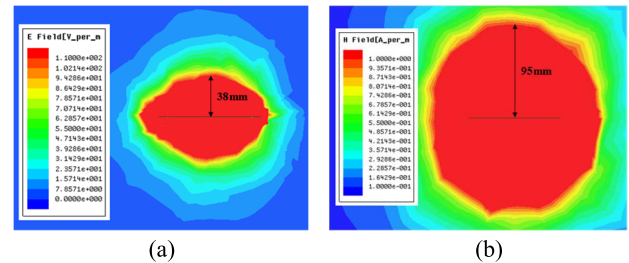


Fig. 26. Side view of field distribution. (a) E-field. (b) H-field.

In addition, the  $z$ -axis was fixed at 1 cm to conduct the experiment. Through this experiment, it was found that the proposed unequal resonator receives power with higher efficiency up to 4 cm from the origin. After 4 cm, the conventional type resonator receives power with higher efficiency, but the efficiency is less than 10%. Operating with a transmission efficiency of less than 10% can cause problems, such as damage to the amplifier or heat generation, due to reflected waves, so it can be interpreted as being out of operation range. Therefore, if the result is checked only within the operating range, it can be seen that the proposed unequal resonator receives power with higher efficiency even on the  $y$ -axis.

In this section, the relationship between  $Q$ -factor and efficiency, and the relationship between each parameter and transmission distance were explained. There were other parameters that were not related to each other. Typically, the transmission power and the proximity resistance were not related.

## V. ACTUAL CELL PHONE CHARGING EXPERIMENT

Using the above results, the actual cell phone charging experiment was performed. The overall experiment consisted of a power meter, an oscilloscope, a power amplifier, and a 40-dB coupler, as shown in Fig. 24. First, the power meter is connected to the forward port of the coupler to read the 6.78-MHz power flowing into the load in real time. Next, the oscilloscope was used to read the current and voltage flowing into the cell phone after passing through the rectifier and the converter. Finally, comparing the results of the power meter and the oscilloscope, we can predict the antenna transmission efficiency and ac-to-dc power conversion efficiency. Fig. 23 shows a block diagram of a charging experiment. Also, the losses incurred in each part are specified. As shown in Fig. 23, the transmission loss is only about 10%, but a total loss of 35% occurs due to return loss and conversion loss. Among these, the return loss can be improved by impedance matching, but the conversion loss is limited in improvement.

The receiver circuit is constructed, as shown in Fig. 24(b). The receiver antenna was also fabricated on the basis of the above results, and the rectifier section was composed of a full-bridge rectifier circuit using a zhcs2000 diode. In addition, the voltage was stabilized using an LM46002.

Fig. 25(a) shows that the power transmitted from the 6.78-MHz power supply to the antenna end is read as 0.3 mW, which is actually taken from the 40-dB coupler, so it can be predicted that 3 W is actually transmitted. In this case, considering the insertion loss of the coupler on the data sheet is 0.5 dB, the actual output can be estimated as 2.7 W. As you can see, the current flowing into the mobile phone is about 400 mA, and the voltage is 4.35 V. As a result, it can be seen that the efficiency is about 65%.

According to [10], in the case of general public/local exposure conditions, the allowable value of the  $H$ -field at 6.78 MHz is less than about  $1 \text{ Am}^{-1}$ , and the allowable value of the  $E$ -field is less than  $110 \text{ Vm}^{-1}$ . If the resonator proposed in this article is powered by 3 W using a simulation tool,  $H$ -field and  $E$ -field are generated, as shown in Fig. 26. Each exceeding the allowable range is 95 mm for  $H$ -field and 38 mm for  $E$ -field. Therefore, if it is used outside 95 mm, it can be used stably without violating the standard. This result is the result of simulation without applying any shielding technology. Therefore, there is room for improvement if shielding techniques, such as [11]–[13], are applied.

## VI. CONCLUSION

A new structure is proposed in this article. In times past, many studies about circular coil antennas are performed. However, because of some disadvantages, the print-based antenna is researched recently. This article also uses a print-based structure. To increase the  $Q$ -factor, an unequal structure is proposed. To support the structure mathematically, modeling of the conventional print-based antenna is performed by a commercial programming tool. Through the commercial programming tool analysis, we can see how the parameters of

the antenna affect the electrical characteristics. Through the result, we can obtain two tendencies. First,  $w$  and  $s$  have some ratios to make the condition of the  $Q$ -factor best. Second, the  $Q$ -factor can be increased by increasing the outer diameter. By these two main results, the optimal unequal structure is developed experimentally. Consequently, the new structure has a higher  $Q$ -factor than the existing structure about 21.8%. In terms of efficiency, the new antenna has better efficiency than the conventional type. We analyzed the unequal structure and investigated what characteristics the width and pitch of the line affect, and through this, we provide an idea to design the optimal printed antenna within the specified design conditions. Through this, the problem of low  $Q$ -factor, which is one of the biggest issues of the existing printed antenna, can be improved. In addition, it can be confirmed that the antenna performance is substantially superior to that of a typical coil antenna if the size conditions are the same. It was confirmed that the printed antenna, which is overwhelmingly advantageous in terms of productivity and reproducibility, can achieve similar performance to the coil antenna.

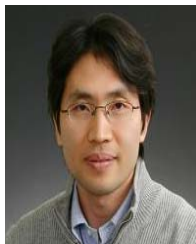
## REFERENCES

- [1] Z. Duan, Y.-X. Guo, and D.-L. Kwong, "Rectangular coils optimization for wireless power transmission," *Radio Sci.*, vol. 47, no. 3, pp. 1–10, Jun. 2012.
- [2] D. C. Ng, C. Boyd, S. Bai, G. Felic, M. Halpern, and E. Skafidas, "High- $Q$  flexible spiral inductive coils," in *Proc. Electromagn. Compat. Symp. (Melbourne)*, Sep. 2010, pp. 1–4.
- [3] S. Y. Kim, T. Y. Kim, and J. R. Choi, "Design of high efficiency resonant coil and receiver IC for wireless power transfer in mobile device," in *Proc. 5th Int. Conf. Modern Circuits Syst. Technol. (MOCAS)*, May 2016, pp. 1–4.
- [4] R. Qin and D. Costinett, "Multi-layer non-uniform series self-resonant coil for wireless power transfer," in *Proc. IEEE Energy Convers. Congr. Expo. (ECCE)*, Sep. 2019, pp. 3333–3339.
- [5] F. Jolani, Y. Yu, and Z. Chen, "A planar magnetically coupled resonant wireless power transfer system using printed spiral coils," *IEEE Antennas Wireless Propag. Lett.*, vol. 13, pp. 1648–1651, 2014.
- [6] K. Chen and Z. Zhao, "Analysis of the double-layer printed spiral coil for wireless power transfer," *IEEE J. Emerg. Sel. Topics Power Electron.*, vol. 1, no. 2, pp. 114–121, Jun. 2013.
- [7] U.-M. Jow and M. Ghovanloo, "Design and optimization of printed spiral coils for efficient transcutaneous inductive power transmission," *IEEE Trans. Biomed. Circuits Syst.*, vol. 1, no. 3, pp. 193–202, Sep. 2007.
- [8] W. B. Kuhn and N. M. Ibrahim, "Analysis of current crowding effects in multilayer spiral inductors," *IEEE Trans. Microw. Theory Techn.*, vol. 49, no. 1, pp. 31–38, Jan. 2001.
- [9] S. Raju, R. Wu, M. Chan, and C. P. Yue, "Modeling of mutual inductance for planar inductors used in inductive link applications," in *Proc. IEEE Int. Conf. Electron Devices Solid State Circuit (EDSSC)*, Dec. 2012, pp. 1–2.
- [10] A. Ahlbom *et al.*, "Guidelines for limiting exposure to time-varying electric, magnetic, and electromagnetic fields (up to 300 GHz)," *Health Phys.*, vol. 74, no. 4, pp. 494–522, Apr. 1998.
- [11] T. Campi, S. Cruciani, F. Maradei, and M. Feliziani, "Near-field reduction in a wireless power transfer system using LCC compensation," *IEEE Trans. Electromagn. Compat.*, vol. 59, no. 2, pp. 686–694, Apr. 2017.
- [12] J. Kim, H. Kim, C. Song, I.-M. Kim, Y.-I. Kim, and J. Kim, "Electromagnetic interference and radiation from wireless power transfer systems," in *Proc. IEEE Int. Symp. Electromagn. Compat. (EMC)*, Raleigh, NC, USA, Aug. 2014, pp. 171–176.
- [13] J. Besnoff, M. Chabalko, and D. S. Ricketts, "A frequency-selective zero-permeability metamaterial shield for reduction of near-field electromagnetic energy," *IEEE Antennas Wireless Propag. Lett.*, vol. 15, pp. 654–657, 2016.



**Jinhyoung Kim** (Student Member, IEEE) received the B.S. degree from Dankook University, Yongin, South Korea, in 2013, and the M.S. degree from Korea University, Seoul, South Korea, in 2015. He is currently pursuing the Ph.D. degree in electrical engineering with Seoul National University, Seoul, with a focus on wireless power transfer and flexible antennas.

Since 2013, he has been a Hardware Research Engineer with Korea Electronics Technology Institute, Seongnam-si, South Korea, working on the development of the Next Generation Convergence Sensor Research Center. He is currently a Fellow Researcher with Korea Electronics Technology Institute. His research areas include mmWave beam focusing/shaping techniques and high-gain antenna for wireless power transfer, and flexible antenna for wearable devices.



**Cheolung Cha** received the B.S. degree in electrical engineering from Korea University, Seoul, South Korea, in 1996, and the M.S. and Ph.D. degrees in electrical and computer engineering (ECE) from Georgia Institute of Technology, Atlanta, GA, USA, from 1998 to 2004.

Since 2004, he has been with the Smart Sensor Research Center, Korea Electronics Technology Institute (KETI), Seongnam-si, South Korea. He has been the Director and a Visiting Professor with the School of Electrical Engineering, Korea University, Seoul, since 2008. His research interests are wireless power transfer technologies, such as inductive coupling, magnetic resonant coupling, and microwave-based beam forming and steering for low-power wearable and IoT device and sensor applications. His other research topic is the radar sensor system.

Dr. Cha received the 53rd IEEE ECTC Outstanding Poster Paper Award in 2004, the SMTA Outstanding Engineer Award in 2008, the IEC Thomas Edison Award in 2015, and the Industrial Technology Award and Medal from Korean Government in 2015. He has been a Secretary of the Technical Committee 47 (Semiconductor devices), International Electrotechnical Commission (IEC), Geneva, Switzerland, since 2007.



**Jungsuek Oh** (Senior Member, IEEE) received the B.S. and M.S. degrees from Seoul National University, Seoul, South Korea, in 2002 and 2007, respectively, and the Ph.D. degree from the University of Michigan, Ann Arbor, MI, USA, in 2012.

From 2007 to 2008, he was a Hardware Research Engineer with Korea Telecom, Seongnam-si, South Korea, working on the development of flexible RF devices. In 2012, he was a Post-Doctoral Research Fellow with the Radiation Laboratory, University of Michigan. From 2013 to 2014, he was a Staff RF Engineer with Samsung Research America, Dallas, TX, USA, working as a Project Leader for the 5G/millimeter-wave antenna systems. From 2015 to 2018, he was a Faculty Member with the Department of Electronic Engineering, Inha University, Incheon, South Korea. He is currently an Associate Professor with the School of Electrical and Computer Engineering, Seoul National University. He has published more than 50 technical journal articles and conference papers. His research areas include mmWave beam focusing/shaping techniques, antenna miniaturization for integrated systems, and radio propagation modeling for indoor scenarios.

Dr. Oh has served as a TPC Member and the Session Chair of the IEEE Antenna and Propagation Society (AP-S)/Ultra Safe Nuclear Corporation (USNC)-International Union of Radio Science (URSI) and the International Symposium on Antennas and Propagation (ISAP). He was a recipient of the 2011 Rackham Predoctoral Fellowship Award at the University of Michigan. He has served as a Technical Reviewer for the IEEE TRANSACTIONS ON ANTENNAS AND PROPAGATION, IEEE ANTENNAS AND WIRELESS PROPAGATION LETTERS, and so on.



**Yongtaek Hong** (Member, IEEE) received the B.S. and M.S. degrees in electronics engineering from Seoul National University, Seoul, South Korea, in 1994 and 1996, respectively, and the Ph.D. degree in electrical engineering from the University of Michigan, Ann Arbor, MI, USA.

From 2003 to 2006, he was a Senior Research Scientist with the Display Science & Technology Center, Eastman Kodak Company, Rochester, NY, USA. Since 2006, he has been with the Department of Electrical and Computer Engineering, Seoul National University, where he is currently a full Professor. He was a Visiting Professor with the Department of Chemical Engineering, Stanford University, Stanford, CA, USA, from 2012 to 2013. His research interests are printed/flexible/stretchable thin-film devices, and display and sensors for wearable and electronic skin applications.

Prof. Hong received the IEEE EDS "2005 George E. Smith Award," the IEEE/IEEK "Young IT Engineer of The Year Award" in 2010, the IEC "1906 Award" in 2012, the "Industrial Technology of the Month Award" and the "KEIT Chairman's Award" from MOTIE of Korean Government in 2014 and 2015, respectively, the SNU CoE Shin Yang Engineering Award in 2015, the Best Academic Development in Printed & Flexible Electronics Award from IDTechEX Show Printed Electronics USA and the 100 Technology Lighting-up Korea in 2025 Award in 2017, the "Display Day" Korea MOTIE Minister Award in 2018, and the "Scientist of The Month" Korea MSIT Minister Award in 2019. He is also a Convenor of IEC TC110 WG8 (Flexible Display Devices), an Executive Board Member of the Korean Information Display Society (KIDS) and the Society for Information Display (SID), and the Chair of the IEEE ED Seoul Chapter and the SID Chapter Formation.